View metadata, citation and similar papers at core.ac.uk
brought to you by CORE
provided by PORTO Publications Open Repository TOrino

An Efficient Approach to Noise Analysis Through Multidimensional Physics-Based Models

Fabrizio Bonani, *Member, IEEE*, Giovanni Ghione, *Senior Member, IEEE*,
Mark R. Pinto, *Senior Member, IEEE*, and R. Kent Smith

***Abstract*— The paper presents a general approach to numerically simulate the noise behavior of bipolar solid-state electron devices through a physics-based multidimensional device model. The proposed technique accounts for noise sources due to carrier velocity and population fluctuations. The power and correlation spectra of the external current or voltage fluctuations are evaluated through a Green's function, linear perturbation theory equivalent to the classical Impedance Field Method for noise analysis and its generalizations. The numerical implementation of the method is performed through an efficient technique, which allows noise analysis to be carried out with negligible overhead with respect to the small-signal simulation. Some case studies are analyzed in order to compare the present approach with theoretical results from the classical noise theory of pn junctions and bipolar transistors.**

I. Introduction

NOISE PERFORMANCES are an important feature of solid-state analog devices. In many analog applications—e.g., front-end microwave and millimeter-wave small-signal amplifiers; low-frequency amplifiers for instrumentation; microwave mixers and oscillators—the noise behavior under linear (small-signal) and nonlinear (large-signal) operation is the main concern of the designer. Moreover, the growing importance of wireless applications in the upper radio-frequency (RF) and lower microwave range, and the potential shown there by silicon-based analog IC's, suggest that the optimization of noise performances will become mandatory not only, as in the past, for GaAs microwave devices, but also for Si RF and microwave active components. Indeed, much effort has been devoted, during the last few decades, to achieve a sound physical understanding of microscopic noise mechanisms within solid-state electron devices—see [1] for a review—and to develop methods to derive, from the semiconductor microscopic noise behavior, the noise characterization of the device, at least in small-signal conditions. Noise device modeling under large-signal operation has been recently the object of great interest, but a full theory for nonlinear noise modeling is still under development [2].

Classical methods for noise analysis make use of a two-step technique. First, they identify a set of microscopic noise sources in terms of carrier velocity and population fluctuations—called *diffusion* and *generation-recombination* noise sources, respectively. Second, they evaluate the effect of microscopic fluctuations on voltage or current fluctuations at the device terminals. Owing to the small amplitude of microscopic fluctuation, this latter task is performed through linear perturbation of the transport model and solution through a Green's function technique. Since fluctuations are zero-average random processes, the final outcome we seek is a statistical, often second-order, characterization of external voltage or current fluctations at the device terminals. This approach, which can be rigourously derived from the master equation formalism [1], is the basis for the impedance field method (IFM) [3] and its variations and generalizations (see e.g., [1] and references therein).

In recent years, with the development of solid-state device numerical modeling, some effort has been devoted to the implementation of the IFM within the framework of numerical device models. Nevertheless, most implementations only concern quasi-two-dimensional (quasi-2-D), semi-analytical, special-purpose applications [4], [5]. On the other hand, little attention was devoted to general-purpose implementations within PDE-based, multidimensional device simulators. A general implementation of the IFM in a 2-D, one-carrier drift-diffusion (DD) simulator based on the *adjoint* approach was proposed in [6] by Ghione *et al.*; however, this technique was not easily extended to two-carrier devices, and only diffusion noise was allowed for. An adjoint-network approach was independently exploited by Layman [7] for the 2-D analysis of MOS devices, including thermal and $1/f$ noise sources.

This work presents a general and comprehensive approach whereby the noise analysis is implemented through a bipolar generalization of the IFM within the framework of the general-purpose, two-carrier, multidimensional simulator PADRE [8]. On the basis of physical, geometrical and process data the simulator provides the frequency-dependent power and correlation spectra of the open-circuit voltage fluctuations at all device ports. The Green's functions implementation derives from *Branin's method* [9] for network noise analysis, which extends and generalizes the adjoint approach. The application of Branin's method allows the noise simulation of the device to be carried out with negligible overhead with respect to the small-signal simulation. The results reported in the paper concern the drift-diffusion model only; however, the extension of the approach to energy-transport or hydrodynamic models is straightforward.

Manuscript received March 18, 1997. The review of this paper was arranged by Editor W. Weber.

F. Bonani and G. Ghione are with the Dipartimento di Elettronica, Politecnico di Torino, 10129 Torino, Italy.

M. R. Pinto and R. K. Smith are with Bell Laboratories, Lucent Technologies, Murray Hill, NJ 07974 USA.

Publisher Item Identifier S 0018-9383(98)00285-8.

0018–9383/98$10.00 © 1998 IEEE

II. Physics-Based Noise Analysis

As discussed in the Introduction, the aim of physics-based noise analysis is the evaluation of the second order statistical properties of the fluctuations at the device terminals induced by the fundamental velocity and population fluctuations occurring throughout the device volume. In small-signal operation, such fluctuations can be assumed to behave as stationary processes, which in turn are effectively represented by the Fourier transform of the correlation functions, namely the *correlation spectra*.

The physical model considered as a basis for the discussion of noise analysis is the bipolar drift-diffusion model

$$\nabla^2\psi = -\frac{q}{\epsilon}(p - n + N^+) \tag{1}$$

$$\frac{\partial n}{\partial t} = \frac{1}{q}\nabla\cdot \underline{J}_n - U_n \tag{2}$$

$$\frac{\partial p}{\partial t} = -\frac{1}{q}\nabla \underline{J}_p - U_p \tag{3}$$

where

- $\psi(\underline{r},t), n(\underline{r},t)$ and $p(\underline{r},t)$ are, respectively, the potential and carrier concentration distributions inside the device;
- N^+ is the net (positive) ionized impurity concentration;
- $\underline{J}_n = qn\mu_n\nabla\psi + qD_n\nabla n$ and $\underline{J}_p = qp\mu_p\nabla\psi - qD_p\nabla p$ are the electron and hole current densities;
- μ and D are the carrier mobility and diffusivity;
- U_n and U_p are the net electron and hole recombination rates, whose expression depends on the generation-recombination mechanisms included in the simulation.

Equations (1)–(3) are completed by suitable boundary conditions (b.c.), including the simulation domain boundaries, the metallic contacts, and the applied bias.

From a mathematical standpoint, the drift-diffusion model can be written as the vector equation

$$\underline{F}(\psi, n, p, \dot{n}, \dot{p}) = 0 \quad \dot{a} = \frac{\partial \alpha}{\partial t}, \alpha = n, p \tag{4}$$

whose solution (ψ_0, n_0, p_0) depends both on the device geometry and on the b.c. In order to perform the noise analysis, a small-amplitude, zero-average stochastic forcing term $\underline{s}(\underline{r},t)$ is added to the right-hand-side (rhs) of (4), thereby yielding a Langevin equation [1]. Velocity fluctuations yield fundamental noise sources in the continuity equations, while GR noise sources result, at least for the Shockley–Read–Hall mechanism, in a noise source term both in the continuity and in the Poisson equations. The perturbed solution has to satisfy the Langevin equation

$$\underline{F}(\psi_0 + \delta\psi, n_0 + \delta n, p_0 + \delta p, \dot{n}_0 + \delta\dot{n}, \dot{p}_0 + \delta\dot{p}) = \underline{s} \tag{5}$$

where $\underline{s}$ represents a *Langevin force* according to the definition in [10]. As a result of the small amplitude of the microscopic noise sources, (5) can be given the following first-order approximation

$$\left.\frac{\partial \underline{F}}{\partial \psi}\right|_0 \delta\psi + \left.\frac{\partial \underline{F}}{\partial n}\right|_0 \delta n + \left.\frac{\partial \underline{F}}{\partial p}\right|_0 \delta p + \left.\frac{\partial \underline{F}}{\partial \dot{n}}\right|_0 \delta\dot{n} + \left.\frac{\partial \underline{F}}{\partial \dot{p}}\right|_0 \delta\dot{p} = \underline{s} \quad . \tag{6}$$

The linearized Langevin (6), which will be the basis of further discussion, is a linear stochastic partial differential equation [11] with deterministic b.c.[1] and stationary (in this case, white: see Section II-A) stochastic forcing term. According to the theory of linear systems (see [13] and references therein), the formal solution of (6) can be expressed as a convolution integral of the distributed source term $\underline{s}$ times a properly defined *Green's function*. Let us define the Green's function $G_\beta^{(\alpha)}(\underline{r},\underline{r}_1;t,t_1)$ as the response[2] of (6) in variable α ($\alpha = \psi, n, p$) to an impulsive source term $\delta(\underline{r}-\underline{r}_1)\delta(t-t_1)$ added to the rhs of equation β ($\beta = \psi, n, p$ for Poisson, electron and hole continuity equations, respectively). The fluctuation $\delta\alpha$ ($\alpha = \psi, n, p$) induced by the source term $\underline{s}$ is thus given by

$$\delta\alpha(\underline{r},t) = \sum_{\beta=\psi,n,p}\int_\Omega\int_{-\infty}^{t} G_\beta^{(\alpha)}(\underline{r},\underline{r}_1;t,t_1) s_\beta(\underline{r}_1,t_1)\, dt_1\, d\underline{r}_1 \tag{7}$$

where Ω is the device domain. This equation can be significantly simplified if the device is operated in small-signal conditions, i.e., when the unperturbed solution (ψ_0, n_0, p_0) is *stationary*. The stationarity assumption, which holds e.g., for a two-port used as a linear amplifier, results in the time-invariance of the linearized model (6), thereby implying

$$G_\beta^{(\alpha)}(\underline{r},\underline{r}_1;t,t_1) = G_\beta^{(\alpha)}(\underline{r},\underline{r}_1;t-t_1)$$

which in turn allows for a frequency-domain analysis. By introducing the time-variable Fourier transform $\tilde{f}(\underline{r},\omega)$ of $f(\underline{r},t)$, (7) is reduced to

$$\delta\tilde{\alpha}(\underline{r},\omega) = \sum_{\beta=\psi,n,p}\int_\Omega \tilde{G}_\beta^{(\alpha)}(\underline{r},\underline{r}_1;\omega)\tilde{s}_\beta(\underline{r}_1,\omega)\, d\underline{r}_1. \tag{8}$$

From (8), the correlation spectrum $S_{\delta\alpha,\delta\beta}(\underline{r},\underline{r}';\omega)$ of fluctuations $\delta\alpha(\underline{r}), \delta\beta(\underline{r}')$, can be recovered as

$$S_{\delta\alpha,\delta\beta}(\underline{r},\underline{r}';\omega) = \sum_{\gamma,\delta=\psi,n,p}\int_\Omega\int_\Omega \tilde{G}_\gamma^{(\alpha)}(\underline{r},\underline{r}_1;\omega) \cdot S_{s_\gamma,s_\delta}(\underline{r}\underline{r}_1,\underline{r}_2;\omega)\tilde{G}_\delta^{(\beta)*}(\underline{r}',\underline{r}_2;\omega)\, d\underline{r}_1\, d\underline{r}_2 \tag{9}$$

where $S_{s_\gamma,s_\delta}(\underline{r}_1,\underline{r}_2;\omega)$ is the correlation spectrum of $s_\gamma(\underline{r}_1), s_\delta(\underline{r}_2)$.

A. Noise Spectra Evaluation

In order to introduce the circuit representation of a noisy device, let us consider a $(N+1)$-terminal structure where one of the terminals, namely $N+1$, is grounded. The fluctuations induced by the fundamental microscopic noise sources can be described by means of a set of *correlated* open-circuit noise voltage generators connected at the N terminals, as shown

[1] If surface GR noise is included, this amounts to a stochastic b.c. on part of the device surface.

[2] It should be noted that (6) has to be completed by a suitable set of b.c., derived by a linearization of the b.c. applied to the complete system (5) and imposed on the linearized model only.

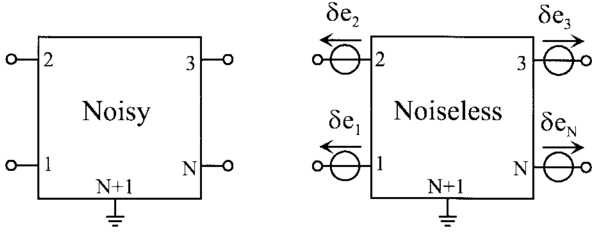

Fig. 1. Circuit representation of a $N+1$)-terminal device.

in Fig. 1. The open-circuit conditions at the device terminals have to be explicitly introduced as b.c. in the Green's functions definition, thus resulting in N auxiliary equations added to the linearized drift-diffusion model. Since we shall deal with the potential Green's functions only, in what follows we shall drop the ψ superscript, so that $\tilde{G}_\alpha^{(\psi)} = \tilde{G}_\alpha$.

Once the Green's functions have been evaluated, the spectra associated to the open-circuit noise voltage generators can be calculated according to the following technique. For the sake of simplicity, we shall derive the noise spectra for microscopic noise sources appearing in the continuity equations only, i.e., we shall consider diffusion noise sources and GR mechanism not involving trap levels. The formulation for SRH GR processes, yielding noise sources also in the Poisson equation, is a straightforward extension. The source term $\underline{s}$ is then given by

$$s_\psi = 0, s_\alpha = \gamma_\alpha + \frac{1}{q}\nabla\cdot\underline{\xi}_\alpha \quad \alpha = n,p$$

where γ_α is the GR noise source and $\underline{\xi}_\alpha$ is the diffusion noise source. Details on the mathematical meaning of such sources can be found in [12]. The open circuit fluctuation $\delta\tilde{e}_i(\omega) = \delta\tilde{\psi}(\underline{r}_i,\omega)$ induced on electrode i, located in $\underline{r}_i$, is given by (8). Careful application of Gauss's theorem neglecting surface microscopic noise sources [13] yields

$$\delta\tilde{e}_i(\omega) = \sum_{\alpha=n,p}\left\{\int_\Omega \tilde{G}_\alpha(\underline{r}_i,\underline{r};\omega)\gamma_\alpha(\underline{r})\, d\underline{r} - \int_\Omega \underline{\tilde{G}}_\alpha(\underline{r}_i,\underline{r};\omega)\cdot\tilde{\underline{\xi}}_\alpha(\underline{r},\omega)\, d\underline{r}\right\} \quad (10)$$

where the *vector* Green's function $\underline{\tilde{G}}$ is defined as

$$\underline{\tilde{G}}_\alpha(\underline{r},\underline{r}_1;\omega) = \frac{1}{q}\nabla_{\underline{r}_1}\tilde{G}_\alpha(\underline{r},\underline{r}_1;\omega) \qquad \alpha = n,p. \quad (11)$$

In (10) the Green's functions $\tilde{G}_\alpha$ are defined as the small-signal potential induced in the device volume by a unit source term in equation α injected in $\underline{r}_1$, provided that open-circuit b.c. at the N device terminals have been enforced. Thus, $\tilde{G}_\alpha$ is the solution of the linear system

$$\begin{aligned}
\nabla^2_{\underline{r}}\tilde{G}_\alpha(\underline{r},\underline{r}_1;\omega) &= -\Lambda_\psi(\tilde{G}_\alpha,\delta\tilde{n},\delta\tilde{p})\\
j\omega\delta\tilde{n}(\underline{r},\underline{r}_1;\omega) &= -\Lambda_n(\tilde{G}_\alpha,\delta\tilde{n},\delta\tilde{p}) + \delta_{\alpha,n}\delta(\underline{r}-\underline{r}_1)\\
j\omega\delta\tilde{p}(\underline{r},\underline{r}_1;\omega) &= -\Lambda_p(\tilde{G}_\alpha,\delta\tilde{n},\delta\tilde{p}) + \delta_{\alpha,p}\delta(\underline{r}-\underline{r}_1)
\end{aligned} \quad (12)$$

where $\delta_{\alpha,\beta}$ is Kronecker's delta and Λ_β is the linear function of its arguments corresponding to the linearization of the drift-diffusion equations around the DC working point.

The Green's function approach to the solution of the Langevin equation is, as shown in [14], equivalent to Shockley's *Impedance Field Method* [3], where the *scalar* impedance field $\tilde{Z}_\alpha$, defined as the open circuit small-signal potential induced by an injected unit-amplitude, spatially impulsive, harmonic scalar electron or hole current source (added to the rhs of the continuity equation for carrier $\alpha = n,p$, respectively), is given by ($\kappa_n = -1, \kappa_p = +1$)

$$\tilde{Z}_\alpha(\underline{r}_i,\underline{r};\omega) = \frac{\kappa_\alpha}{q}\tilde{G}_\alpha(\underline{r}_i,\underline{r};\omega) \qquad \alpha = n,p. \quad (13)$$

A similar relation holds also for the *vector* impedance field $\underline{\tilde{Z}}_\alpha$, defined in [3] as the open circuit small-signal potential induced by a unit-amplitude, spatially impulsive, harmonic injected (vector) current density source

$$\underline{\tilde{Z}}_\alpha(\underline{r}_i,\underline{r};\omega) = \nabla_{\underline{r}}\tilde{Z}_\alpha(\underline{r}_i,\underline{r};\omega) = \kappa_\alpha\underline{\tilde{G}}_\alpha(\underline{rr}_i,\underline{r};\omega) \quad \alpha = n,p. \quad (14)$$

The correlation spectrum between the noise generators δe_i and δe_j can be derived from (9); however, microscopic noise sources are often assumed as spatially uncorrelated, thus leading to the source correlation spectra

$$S_{\gamma_\alpha,\gamma_\beta}(\underline{r},\underline{r}_1;\omega) = K_{\gamma_\alpha,\gamma_\beta}(\underline{r},\omega)\delta(\underline{r}-\underline{r}_1) \quad (15)$$

$$\underline{\underline{S}}_{\underline{\xi}_\alpha,\underline{\xi}_\beta}(\underline{r},\underline{r}_1;\omega) = \underline{\underline{K}}_{\underline{\xi}_\alpha,\underline{\xi}_\beta}(\underline{r},\omega)\delta(\underline{r}-\underline{r}_1) \quad (16)$$

where K and $\underline{\underline{K}}$ are the *microscopic local noise sources* for GR and diffusion noise processes defined by Nougier [16], whose expression depends on the physical mechanisms involved in the fundamental fluctuations. Owing to the delta dependence of the source correlation spectra, (9) simplifies into

$$\begin{aligned}
S_{\delta e_i,\delta e_j}(\omega) &= \sum_{\alpha,\beta=n,p}\int_\Omega \tilde{G}_\alpha(\underline{r}_i,\underline{r};\omega)K_{\gamma_\alpha,\gamma_\beta}(\underline{r};\omega)\tilde{G}^*_\beta(\underline{r}_j,\underline{r};\omega)\, d\underline{r}\\
&\quad + \sum_{\alpha,\beta=n,p}\int_\Omega \underline{\tilde{G}}_\alpha(\underline{r}_i,\underline{r};\omega)\\
&\quad \cdot\underline{\underline{K}}_{\underline{\xi}_\alpha,\underline{\xi}_\beta}(\underline{r};\omega)\cdot\underline{\tilde{G}}^\dagger_\beta(\underline{r}_j,\underline{r};\omega)\, d\underline{r}
\end{aligned} \quad (17)$$

which is the classical IFM expression of noise [3], [15].

A rigorous mathematical foundation for the correlation spectra of the noise sources in (15) and (16) can be found in [12]. For band-to-band GR processes, the local noise source is given by

$$\begin{aligned}
K_{\gamma_n,\gamma_n} &= 2(R_n + G_n)\\
K_{\gamma_p,\gamma_p} &= 2(R_p + G_p)\\
K_{\gamma_n,\gamma_p} &= K_{\gamma_p,\gamma_n} = -2(R_n + G_n) = 2(R_p + G_p)
\end{aligned} \quad (18)$$

where R_α and G_α are, respectively, the recombination and generation rates for carrier α ($\alpha = n,p$) in the DC operating point. Carrier velocity fluctuations are instead represented as current density local noise sources, whose spectra is proportional to the carrier diffusivity tensor $\underline{\underline{D}}_\alpha$

$$\begin{aligned}
\underline{\underline{K}}_{\underline{\xi}_n,\underline{\xi}_n} &= 4q^2 n\underline{\underline{D}}_n\\
\underline{\underline{K}}_{\underline{\xi}_p,\underline{\xi}_p} &= 4q^2 p\underline{\underline{D}}_p\\
\underline{\underline{K}}_{\underline{\xi}_n,\underline{\xi}_p} &= \underline{\underline{K}}_{\underline{\xi}_p,\underline{\xi}_n} = 0
\end{aligned} \quad (19)$$

where all quantities are evaluated in DC conditions.

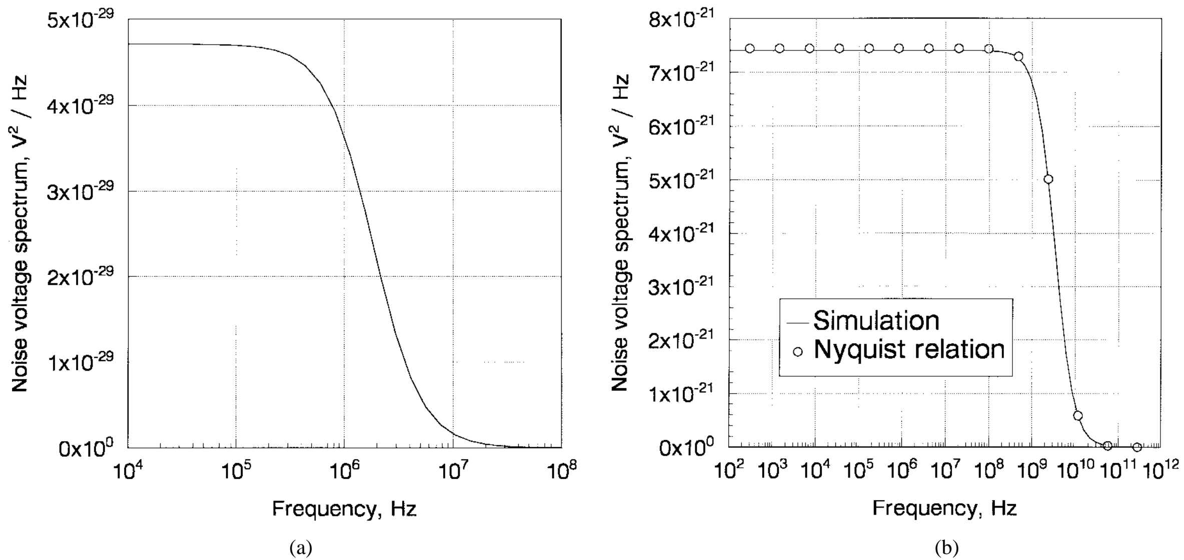

Fig. 2. Frequency dependence of (a) the GR voltage noise spectrum and (b) the diffusion noise spectrum for a uniformly-doped semiconductor sample. The open circles are calculated according to the Nyquist relation.

III. The Numerical Approach

In order to apply (17), the evaluation of the scalar Green's functions $\tilde{G}_\alpha$ through a numerical solution of (12) is required. Let us assume that a mesh with N_p points has been defined on the device volume, and that the device equations have been correspondingly discretized by means of the finite boxes technique [17]. According to (17), the Green's functions need to be evaluated only for the N observation points $\underline{r}_i$ corresponding to the open-circuited terminals,[3] and not for all the N_p mesh points.

To evaluate the open-circuit fluctuations, (12) has to be completed by N auxiliary equations enforcing AC open circuit b.c. at the device electrodes, thereby requiring to introduce the electrode AC potentials $\underline{V} = \{V_k\}^T (k = 1, \cdots, N)$ as auxiliary unknowns. The discretized linear system is then

$$\begin{bmatrix} \underline{\underline{J}}_c & \underline{\underline{B}}_x \\ \underline{\underline{A}}_x^T & \underline{\underline{D}}_x \end{bmatrix} \begin{bmatrix} \underline{\underline{y}} \\ \underline{\underline{V}} \end{bmatrix} = \begin{bmatrix} \underline{\underline{P}}_j \\ 0 \end{bmatrix} \tag{20}$$

where

- $\underline{\underline{J}}_c$ is the small-signal matrix (dimension $3N_p \times 3N_p$ for a bipolar simulation) of the model, including the b.c. following from the linearization of the full system b.c.;
- $\underline{\underline{A}}_x^T$ $(N \times 3N_p)$, $\underline{\underline{D}}_x$ $(N \times N)$ are matrices enforcing the open circuit b.c. at the N device terminals;
- $\underline{\underline{B}}_x$ $(3N_p \times N)$ is a matrix linking the internal unknowns $\underline{\underline{y}}$ to the auxiliary unknowns $\underline{\underline{V}}$;
- $\underline{\underline{P}}_j$ is a matrix $(3N_p \times 2N_p)$ each of whose columns has only one nonzero entry, corresponding to the finite-boxes discretization of the spatial delta function in each of the continuity equations [see (12)];
- $\underline{\underline{y}}$ $(3N_p \times 2N_p)$ and $\underline{\underline{V}}$ $(N \times 2N_p)$ are unknown matrices, the first representing the potential and carrier concentration distributions, the second containing the electrode potentials.

[3] Although several mesh nodes are typically used to discretize each device terminal, they are forced to be equipotential. The Green's function definition is therefore unambiguous.

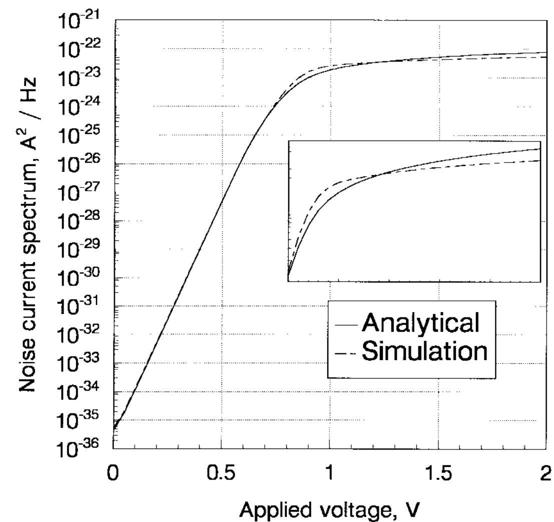

Fig. 3. Comparison between the bias dependence of the analytical and simulated noise current spectrum of a 2-D diode ($f = 10$ kHz).

As already remarked, only $\underline{\underline{V}}$ has to be evaluated. In fact, the Green's functions for the i-th electrode (observation point $\underline{r}_i, i = 1, \cdots, N$) is the ith row of $\underline{\underline{V}}$.

A direct solution of (20) would require, at least for a bipolar model, $2 \times N_p$ backsolves once the full system matrix has been factorized. We have developed an efficient numerical technique, based on Branin's approach to the noise simulation of large electrical networks [9], which allows for the evaluation of the Green's functions with just N backsolves—i.e., two for a three-terminal device as a BJT or FET—of a properly defined transposed linear system [18], [15]. On substituting the first equation of (20) in the second one, one obtains that $\underline{\underline{V}} = \underline{\underline{T}}\,\underline{\underline{P}}_j$, where $(N \times 3N_p)$ is a matrix whose columns are

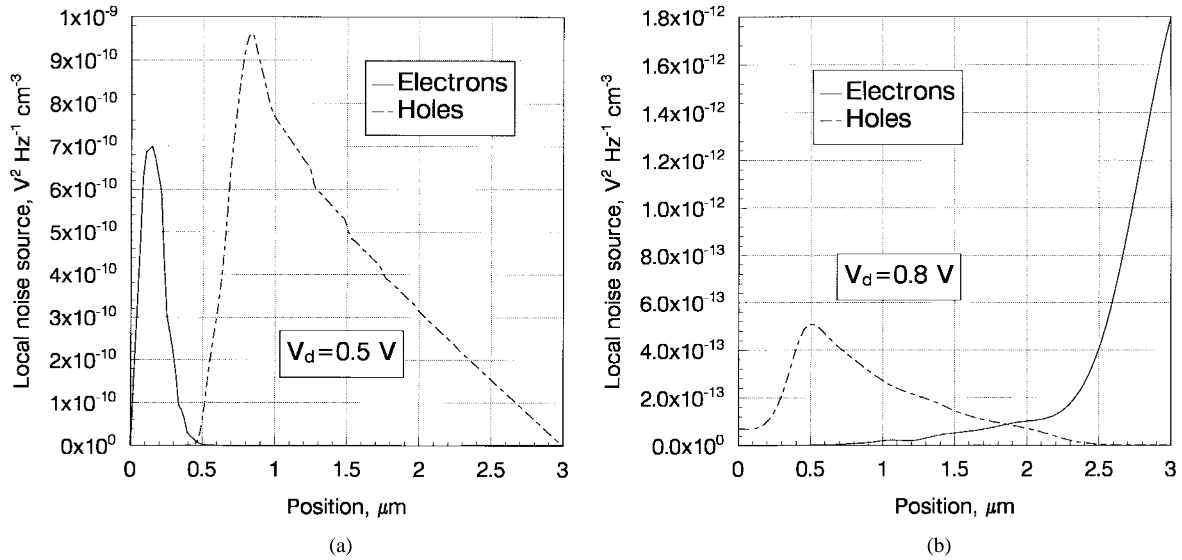

Fig. 4. Depth dependence (section for $x = 0.25$ μm) of the distributed local noise source ($f = 10$ kHz) for the 2-D diode in low-injection [$V_d = 0.5$ V, (a)] and high-injection [$V_d = 0.8$ V, (b)].

defined by the N-fold linear system

$$(\underline{\underline{D}}_x - \underline{\underline{y}}_0^T \underline{\underline{B}}_x)\underline{\underline{T}} = -\underline{\underline{y}}_0^T \tag{21}$$

whose rhs is solution of

$$\underline{\underline{J}}^T_c \underline{\underline{y}}_0 = \underline{\underline{A}}_x \tag{22}$$

involving the small-signal transposed matrix of the linearized model only. The solution algorithm is then as follows.

1) $\underline{\underline{y}}_0$ $(3N_p \times N)$ is evaluated solving (22). This has the same computational burden as N small-signal analyzes.
2) $\underline{\underline{T}}$ $(N \times 3N_p)$ is evaluated solving (21), with a negligible overhead on the computational intensity.
3) The Green's functions are evaluated through the product $\underline{\underline{V}} = \underline{\underline{T}}\ \underline{\underline{P}}_j$.

Besides the obvious reduction in the computational intensity, another advantage of this approach is that it can be directly extended to any PDE-based device model and to any of the Green's functions defined in Section II.

IV. Examples

The efficient numerical technique for the evaluation of the Green's functions has been implemented in a general-purpose device simulator (PADRE [8]) allowing for the solution of the drift-diffusion and energy-balance models in one, two or three spatial dimensions for a device with an arbitrary number of electrodes. The noise model has been developed for the drift-diffusion model only, although the numerical technique can be extended to a PDE-based model of any order.

A. Uniformly-Doped Sample

As a first example of application of noise analysis, we present a one-dimensional simulation of a uniformly-doped semiconductor sample. The sample is 100 μm long, the n-type doping level is 10^{14} cm^{-3}, and a band-toband GR process has been taken into account with a recombination lifetime of 100 ns. Fig. 2 shows the frequency dependence of the (a) GR and (b) diffusion components of the open-circuit noise voltage spectrum $S_{\delta\tilde{e},\delta\tilde{e}}(f)$ for an electric field of 10 V/cm. As expected, the GR component shows a Lorentzian frequency dependence whose corner angular frequency is related, but not equal to, the reciprocal of the recombination lifetime. This behavior is due to the influence of the b.c. imposed by the ohmic contacts at the device terminals on the Green's functions. A detailed analysis is beyond the scope of this paper, but a significant remark can be nevertheless drawn: GR microscopic noise sources have been traditionally included in device simulation by means of an equivalent noise source described in terms of current density fluctuations, wherein the Lorentzian frequency dependence is already included in the noise source itself [16]. This approximation requires the introduction of a heuristical electric-field dependence both in the corner frequency and in the low-frequency value of the equivalent noise source in order to fit the experimental results, while the Langevin source (18) is white. In the latter case, the frequency and electric field dependence of the external noise voltage spectrum is due to a complex interplay between the electron and hole scalar Green's functions. Further details can be found in [19].

The diffusion component of the open circuit noise voltage spectrum is in excellent agreement with the theoretical expression (Nyquist equation)

$$S_{\delta e,\delta e}(f) = 4k_B T\,\mathrm{Re}\{Z(f)\}$$

where k_B is Boltzmann constant, T the absolute temperature and $Z(f)$ the small-signal impedance of the device. The agreement is good also in the high frequency limit, where the noise spectrum exhibits a low-pass behavior related to the geometric (parasitic) capacitance of the resistor.

B. 2-D pn Diode

The second simulation example is a 2-D pn diode obtained by a p-type implant (peak concentration of 5×10^{17} cm^{-3}) on

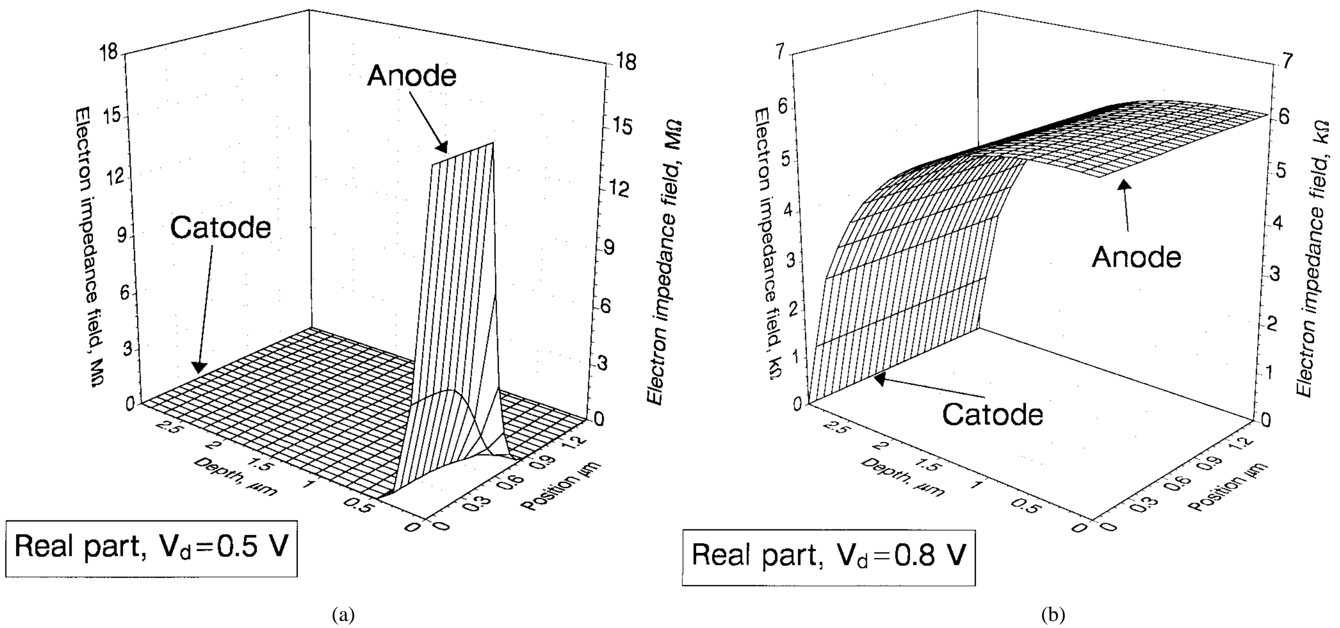

Fig. 5. Real part ($f = 10$ kHz) of the electron impedance field for a 2-D diode in low-injection [$V_d = 0.5$ V, (a)] and high-injection [$V_d = 0.8$ V, (b)].

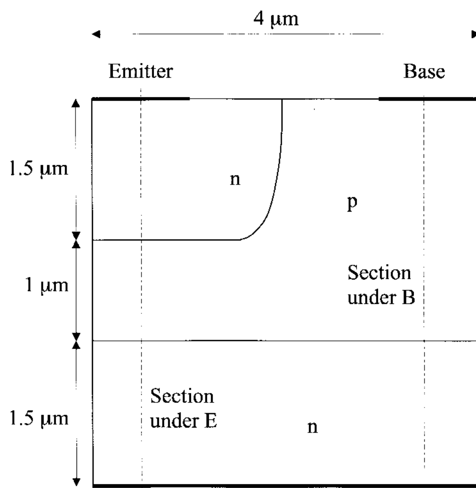

Fig. 6. Cross section of the simulated npn BJT.

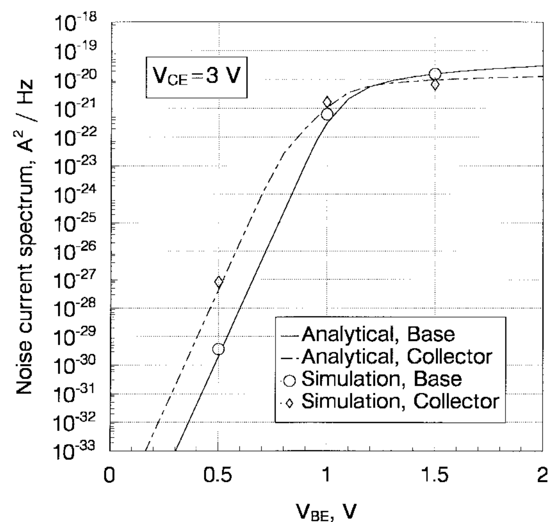

Fig. 7. Comparison between the base bias dependence of the analytical and simulated base and collector noise current spectrum of a 2-D npn BJT ($f = 10$ kHz).

a uniformly-doped n-type ($N_D = 2 \times 10^{15}$ cm^{-3}) substrate so as to obtain a 0.5-μm deep junction. The device is 3 μm wide and 3 μm deep, but for the sake of simplicity, only half device has been simulated—discretized with 800 grid points—so as to reduce the computational intensity.

The theory of noise in arbitrary multidimensional junctions has been developed in [13] under low-injection conditions exploiting the Langevin equation-Green's function approach. The short-circuit noise current follows the shot-like law (indicated as "analytical" in Fig. 3)

$$S_{\delta i,\delta i}(f) = -2qI + 4k_BT\,\mathrm{Re}\{Y(f)\} \approx 2q(I + 2I_0)$$

where I is the DC diode current, $Y(f)$ the small-signal admittance and I_0 the reverse saturation current. The approximation in the previous equation holds if the operating frequency is low enough to neglect frequency dispersion in $\mathrm{Re}\{Y(f)\}$. The simulated noise current spectrum at low frequency ($f = 10$ kHz, see Fig. 3) is in excellent agreement with the theory, while discrepancies arise, as expected, at the onset of high injection. Moreover, a by-product of the Green's function approach is the so-called *local noise source*, i.e., the integrand function of (17), which yields the spatial distribution of noise sources, shown in Fig. 4 both for low [(a), $V_d = 0.5$ V] and for high [(b), $V_d = 0.8$ V] injection conditions. As foreseen by the theoretical analysis, at low injection the spatial noise source for either carrier roughly follows the distribution of excess minority carriers, while at high injection this simple picture is not valid any more. This behavior needs to be explained, because the microscopic local noise source $\underline{\underline{K}}$ is proportional to the sum of the product between each carrier concentration and its diffusivity [see (19)], thus suggesting that majority carriers should play a major role in noise generation.

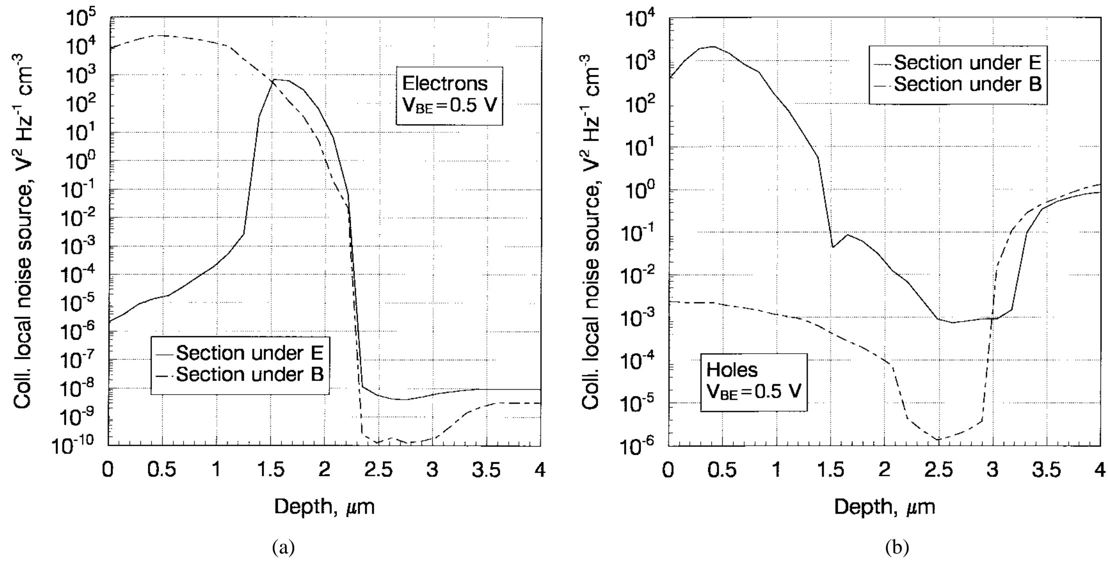

Fig. 8. Sections under base and emitter of the distributed collector local noise source ($f = 10$ kHz) for the 2-D npn BJT in low-injection ($V_{\rm BE} = 0.5$ V), (a) electron and (b) hole components. The collector bias is $V_{CE} = 3$ V.

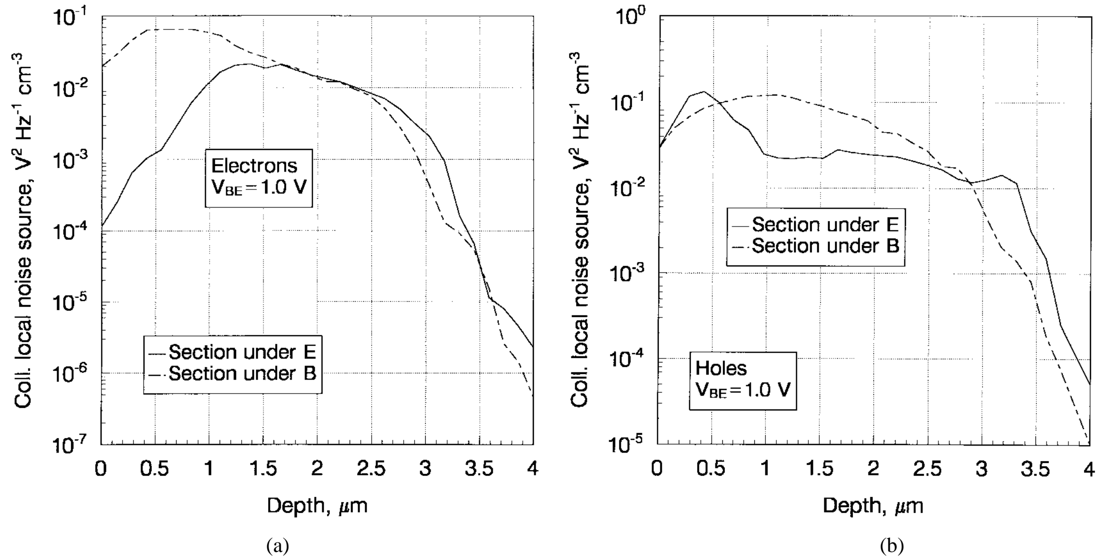

Fig. 9. Sections under base and emitter of the distributed collector local noise source ($f = 10$ kHz) for the 2-D npn BJT in high-injection ($V_{\rm BE} = 1.0$ V), (a) electron and (b) hole components. The collector bias is $V_{CE} = 3$ V.

In fact, the local noise source includes also the gradient of the scalar Green's functions—i.e., the vector Green's functions. Fig. 5 shows the real part of the electron impedance field [proportional to the scalar Green's function through (13)] in (a) low and (b) high injection. In low injection, the scalar Green's function is flat in the n region of the device, and therefore the vector Green's function is not zero only in the p-type region. This picture does not hold anymore in high injection—see Fig. 5(b)—thus explaining the spreding of the local noise source in the majority carrier regions shown in Fig. 4(b). In both cases, the local noise source confirms that, despite its shot-like model, noise in pn diodes does not originate from carrier injection in the space charge region. It may be further noticed that the local noise source due to injected minority carriers is about the same order of magnitude in both sides of the junction, despite the large difference in doping; this suggests that the higher injection efficiency of holes into the n substrate is compensated by the larger magnitude of the electron vector impedance field in the p region.

C. 2-D npn BJT

The last example is a 2-D simulation of a two-port device: an implanted silicon npn bipolar transistor, whose cross section is shown in Fig. 6. The device structure is as follows: a p-type implant (peak concentration: 10^{18} cm^{-3}) is performed on a 4-μm deep uniformly-(n-type)-doped substrate ($N_D = 10^{15}$ cm^{-3}). The corresponding base-collector junction is 2.5 μm deep. The emitter-base junction is then formed, 1.5 μm deep, by a further n-type implantation (peak concentration: 10^{20} cm^{-3}). The emitter implantation is masked so as to allow for a surface base contact (1 μm wide) at the upper right corner of the device. The total device width is 8 μm, but in

order to reduce the numerical burden only half of the structure is simulated, wherein the emitter contact (1 μ μm wide) is placed at the left corner of the upper surface. The collector contact, finally, covers the whole bottom surface 4 μm wide). The discretization grid is made of 1300 points.

According to the general theory developed in [13], in low injection conditions the short-circuit current noise spectra at the base and collector electrodes are given by

$$S_{\delta i_b,\delta i_b}(f) = -2qI_B + 4k_BT\,\mathrm{Re}\{Y_{bb}(f)\}$$
$$S_{\delta i_c,\delta i_c}(f) = -2qI_C + 4k_BT\,\mathrm{Re}\{Y_{cc}(f)\}$$

where $Y_{bb}(f)$ and $Y_{cc}(f)$ are the AC small-signal base and collector admittance, and I_B and I_C are the DC base and collector current, respectively. At low frequency and for negligible parasitic resistances, the customary shot-like expressions are recovered as $S_{\delta i_b,\delta i_b} \approx 2qI_B, S_{\delta i_c,\delta i_c} \approx 2qI_C$, respectively.

As for the pn diode, this behavior is confirmed by the simulations. Fig. 7 shows a comparison between theoretical predictions and simulations for three bias points, one in low-injection ($V_{\rm BE} = 0.5$ V) and the other two in high-injection ($V_{\rm BE} = 1.0$ V and $V_{\rm BE} = 1.5$ V) for the base-emitter junction. The frequency is $f = 10$ kHz.

The physical interpretation of the simulation results follows the same pattern already outlined for the pn diode: in low-injection, noise is due to the minority carriers in each device region—see Fig. 8(a) for the electron and (b) hole local noise source for the collector contact at $V_{\rm BE} = 0.5$ V. Again, this is due to the behavior of the scalar Green's functions, which are flat in the device regions where the corresponding carrier is the majority carrier. Also in the transistor case, the local noise source due to holes injected from the base into the emitter is about the same order of magnitude as the one due to electrons injected through the base, despite the high emitter efficiency, because of the magnitude of the corresponding vector Green's functions. In high-injection the local noise source becomes dominated by majority carriers, see Fig. 9 for the (a) electron and (b) hole local noise source for the collector contact at $V_{\rm BE} = 1.0$ V; however, the resulting short-circuit noise current spectra still exhibit a shot-like behavior.

V. Conclusion

A general approach has been demonstrated for the noise analysis of multidimensional bipolar devices through physics-based numerical modeling. Besides providing, on a set of typical semiconductor devices, results in excellent agreement with theoretical estimates from classical noise theory, the present approach enables to achieve a far better insight on the nature and the origin of external noise in complex, bipolar devices. The general-purpose implementation developed in the paper, besides its computational efficiency, can be readily extended to high-order PDE-based models.

References

[1] C. M. van Vliet, "Macroscopic and microscopic methods for noise in devices," *IEEE Trans. Electron Devices*, vol. 41, pp. 1902–1915, Nov. 1994.

[2] F. Bonani, G. Ghione, S. Donati, L. Varani, and L. Reggiani, "A general framework for the noise analysis of semiconductor devices operating in nonlinear (large-signal quasiperiodic) conditions," in *Proc. 14th Int. Conf. Noise in Phys. Syst. and $1/f$ Fluctuations*, C. Claeys and E. Simoen, Eds. Singapore: World Scientific, 1997, pp. 144–147.

[3] W. Shockley, J. A. Copeland, and R. P. James, "The impedance field method of noise calculation in active semiconductor devices," in *Quantum Theory of Atoms, Molecules, and the Solid-State*, P.-O. Lowdin, Ed. New York: Academic, 1966.

[4] H. A. Haus, H. Statz and R. A. Pucel, "Noise characteristics of gallium arsenide field-effect transistors," *IEEE Trans. Electon Devices*, vol. ED–21, pp. 549–562, 1974.

[5] H. Happy and A. Cappy, *HELENA: HEMT Electrical Properties and Noise Analysis. Software and User's Manual*. Boston, MA: Artech House, 1995.

[6] G. Ghione and F. Filicori, "A computationally efficient unified approach to the numerical analysis of the sensitivity and noise of semiconductor devices," *IEEE Trans. Computer-Aided Design*, vol. 12, pp. 425–438, 1993.

[7] P. A. Layman, "The analysis of thermal and $1/f$ noise in MOS devices, circuits and systems," Ph.D. dissertation, Univ. Waterloo, Waterloo, Ont., Canada, 1989.

[8] M. R. Pinto, C. S. Rafferty, R. K. Smith, and J. Bude, "ULSI Technology development by predictive simulation," in *IEDM Tech. Dig.*, 1993, pp. 701–704.

[9] F. H. Branin, "Network sensitivity and noise analysis simplified," *IEEE Trans. Circuit Theory*, vol. CT-20, pp. 285–288, May 1973.

[10] *Encyclopaedia of Mathematics*. Dordrecht, Germany: Kluwer, vol. 5, p. 347.

[11] K. Sobczyk, *Stochastic Differential Equations*. London, U.K.: Kluwer, 1991.

[12] K. M. van Vliet, "Markov approach to density fluctuations due to transport and scattering. I. Mathematical formalism," *J. Math. Phys.*, vol. 12, no. 9, pp. 1981–1998, Sept. 1971.

[13] ——, "General transport theory of noise in pn junction-like devices—Part I: Three-dimensional Green's function formulation," *Solid-State Electron.*, vol. 15, no. 10, pp. 1033–1053, 1972.

[14] T. C. McGill, M.-A. Nicolet, and K. K. Thornber, "Equivalence of the Langevin method and the impedance-field method of calculating noise in devices," *Solid-State Electron.*, vol. 17, pp. 107–108, 1974.

[15] F. Bonani, G. Ghione, M. R. Pinto, and R. K. Smith, "A novel implementation of noise analysis in general-purpose PDE-based semiconductor device simulators," in *IEDM Tech. Dig.*, 1995, pp. 777–780.

[16] J.-P. Nougier, "Fluctuations and noise of hot carriers in semiconductor materials and devices," *IEEE Trans. Electron Devices*, vol. 41, pp. 2034–2049, Nov. 1994.

[17] R. E. Bank, D. J. Rose, and W. Fichtner, "Numerical methods for device simulation," *IEEE Trans. Electron Devices*, vol. ED-30, pp. 1031–1041, Sept. 1983.

[18] F. Bonani, M. R. Pinto, R. K. Smith, and G. Ghione, "An efficient approach to multidimensional impedance field noise simulation of bipolar devices," in *Proc. 13th Int. Conf. Noise Phys. Syst. and $1/f$ Fluctuations*, V. Bareikis and R. Katilius, Eds. Singapore: World Scientific, 1995, pp. 379–382.

[19] F. Bonani and G. Ghione, "I.F. modeling of GR noise in bipolar devices in terms of fundamental or equivalent microscopic noise sources," in *Proc. 14th Int. Conf. Noise in Phys. Syst. and $1/f$ Fluctuations*, C. Claeys and E. Simoen, Eds. Singapore: World Scientific, 1997, pp. 122–125.

Fabrizio Bonani (S'89–M'96) was born in Torino, Italy, in 1967. He received the Laurea degree, cum laude, and the Ph.D. degree in electronic engineering from Politecnico di Torino, Italy, in 1992 and 1996, respectively.

Since 1995, he has been a Researcher in the Electronics Department, Politecnico di Torino. His research interests are mainly devoted to the physics-based simulation of semicondutor devices, with special emphasis on the noise analysis of microwave field-effect and bipolar transistors, and to the thermal analysis of power microwave circuits. Part of his research concerns the analysis and simulation of nonlinear dynamical systems. From October 1994 to June 1995, he was with the ULSI Technology Research Department of Bell Laboratories, Murray Hill, NJ, as a consultant, working on physics-based noise modeling of electron devices.

Dr. Bonani is member of Associazione Elettrotecnica Italiana (AEI).

Giovanni Ghione (M'87–SM'94) was born in Alessandria, Italy, in 1956. He received the degree, cum laude, in electronic engineering from Politecnico di Torino, Italy, in 1981.

In 1983, he joined Politecnico di Torino as a Research Assistant. From 1987 to 1990, he was an Associate Professor at Politecnico di Milano. In 1990, he joined the University of Catania as Full Professor of Electronics, and, since 1991, he has held the same position at Politecnico di Torino. Since 1981, he has been engaged in Italian and European research projects (ESPRIT 255, COSMIC, and MANPOWER) in the field of active and passive microwave CAD. His present research interests concern the physics-based simulation of active microwave and optoelectronic devices, with particular attention to noise modeling, thermal modeling,and active device optimization. His research interests also include several topics in computational electromagnetics, including coplanar component analysis. He has published more than 100 papers and book chapters in the above fields.

Dr. Ghione is a member of the Editorial Board of IEEE TRANSACTIONS ON MICROWAVE THEORY AND TECHNIQUES, and is a member of the Associazione Elettrotecnica Italiana (AEI).

Mark R. Pinto (S'84–M'84–SM'96) received the B.S. degrees in electrical engineering and computer science from Rensselaer Polytechnic Institute, Troy, NY, and the M.S. and Ph.D. degrees in electrical engineering from Stanford University, Stanford, CA.

He has held summer positions at Hughes Aircraft Company, Rockwell International, IBM Research, and AT&T Bell Laboratories, all in integrated circuit R&D. Since 1985, he has been with Bell Laboratories, Lucent Technologies, Murray Hill, NJ, where he has conducted research primarily in the areas of semiconductor technology and computational device physics. He is currently Director of the Silicon Electronics Research Laboratory, which is responsible for advanced R&D in materials, processes, devices, and IC design in support of communications and information processing businesses in Lucent Technologies.

Dr. Pinto is a recipient of the Bell Laboratories Distinguished Member of Technical Staff Award in 1991 and was selected a Bell Laboratories Fellow in 1995. He is a member of Tau Beta Pi and Eta Kappa Nu.

R. Kent Smith, photograph and biography not available at the time of publication.